IEEE Access
Multidisciplinary | Rapid Review | Open Access Journal

Received March 22, 2022, accepted April 14, 2022, date of publication April 26, 2022, date of current version May 2, 2022.

Digital Object Identifier 10.1109/ACCESS.2022.3169480

A Linear Stochastic Formulation for Distribution Energy Management Systems Considering Lifetime Extension of Battery Storage Devices

ALI SOLEIMANI[1], VAHID VAHIDINASAB[2], (Senior Member, IEEE), AND JAMSHID AGHAEI[3], (Senior Member, IEEE)

[1]Faculty of Electrical Engineering, Shahid Beheshti University, Tehran 1983969411, Iran
[2]Department of Engineering, School of Science and Technology, Nottingham Trent University, Nottingham NG11 8NS, U.K.
[3]LUT School of Energy Systems, Lappeenranta–Lahti University of Technology (LUT), 53850 Lappeenranta, Finland

Corresponding author: Jamshid Aghaei (jamshid.aghaei@lut.fi)

ABSTRACT Recently, the number of Battery Energy Systems (BESs) connected to the grid has grown significantly. These assets can alleviate some operational issues such as demand surges and occasional power fluctuations associated with the Renewable Energy Sources (RESs) connected to the grid. Nonetheless, both overcharging and frequent usage severely affect their health status and shorten their life expectancy. In this paper, an Energy Management System (EMS) framework with a linearised algorithm and in-depth analysis on BES life extension is presented, which optimises the techno-economic aspects of an Active Distribution Network (ADN) connected to RESs. By applying a mathematical linearisation formulation, a Mixed-Integer Linear Programming (MILP) model is proposed for linearising the Optimal Power Flow (OPF) problem. This technique, which has the merit of fair accuracy while having high speed, is used for scheduling BESs to increase their durability and decrease grid costs. To consider the inherent uncertainty associated with demand and RES generation, a two-stage Stochastic Programming (SP) method is implemented in the proposed model. In terms of battery Loss of Health (LoH) assessment, a linearised battery lifetime method is introduced. Ultimately, a modified 33-bus radial distribution test system with a day-ahead Real-Time Pricing (RTP) program was chosen to apply the proposed algorithm and assess its efficiency.

INDEX TERMS Energy management system (EMS), optimal power flow (OPF), linearised AC-OPF, battery scheduling, battery degradation, rain-flow cycle counting, day-ahead pricing.

NOMENCLATURE

A. INDICES & SETS

t	Indice of time interval.
t, n	Indices of time intervals/number of days.
ω, bat	Indices of scenarios/energy storage systems.
i, j, k	Indices of network buses.
X, Y	Indices for lifetime curve piecewise linearisation.
Ω^T, Ω^ω	Sets of time intervals/scenarios.
Ω^{bat}, Ω^B	Sets of network buses/energy storage systems.
$\Lambda^{DoD}, \Lambda^{CtoF}$	Horizontal and vertical axes sets for piecewise linearisation of battery lifetime curve.

B. PARAMETERS

R_{ij}, X_{ij}, Z_{ij}	Resistance/Reactance/Impedance of the line between bus i and j $[\Omega]$.
$P^{load}_{i,t,\omega}, Q^{load}_{i,t,\omega}$	Active and reactive load demand in bus i in scenarioω at time t $[kW]$.
$\overline{V}, \underline{V}$	Maximum/minimum limits of bus voltages $[V]$.
$\overline{I_{ij}}$	Maximum limit of line current between bus i and j $[Amp]$.
$\overline{SoC}, \underline{SoC}$	Maximum/Minimum state of charge limit of energy storage systems $[kW]$.
$\overline{P^{ch}}, \overline{P^{dch}}$	Maximum charging/discharging limit of energy storage systems. $[kW]$.
η^{ch}, η^{dch}	Charging/Discharging efficiency of energy storage systems [-].
$Price_{i,t}$	Electricity unit price of substation located in bus i at time t $[\$/kW]$.

The associate editor coordinating the review of this manuscript and approving it for publication was Binit Lukose.

C^{BES}_{bat}	Purchasing cost of *bat* energy storage system [$].
λ	Piecewise linearisation segments for linearising AC-OPF model [-].
p_ω	Probability of scenario ω [-].

C. BINARY VARIABLES

$q_{ij,t,\omega}$	Line power exchange between bus i and j [-].

D. VARIABLES

OF	Expected objective function value [$].
$Cost^{Net}_{\omega}$	Network operating cost in scenario ω [$].
$Cost^{BES}$	operating cost of energy storage systems in the simulation horizon [$].
$P^{ss}_{i,t,\omega}$, $Q^{ss}_{i,t,\omega}$	Active/Reactive power distributed from Substation on bus i in scenario ω at time t $[kW/kVar]$.
$P_{ij,t,\omega}$, $Q_{ij,t,\omega}$	Active/Reactive power transmitted from bus i to j in scenario ω at time t $[kW/kVar]$.
$I_{ij,t,\omega}$	Current of bus i to j in scenario ω at time t $[Amp]$.
$V_{i,t,\omega}$	Voltage of bus i in scenario ω at time t $[V]$.
$\Delta V_{ij,t,\omega}$	Voltage difference of bus i and j in scenario ω at time t $[V]$.
$P^{ch}_{bat,t}$, $P^{dch}_{bat,t}$	Charging/Discharging Power of *bat* energy storage system at time t $[kW]$.
$SoC_{bat,t}$	State of charge of *bat* energy storage system at time t [-].
$f_{ij,t,\omega}$	Current Squared of bus i to j in scenario ω at time t $[Amp^2]$.
$u_{i,t,\omega}$	Voltage Squared of bus i in scenario ω at time t $[V^2]$.
η, ζ	Auxiliary variables for linearisation [-].
$DOD_{bat,t,n}$	Depth of discharge of *bat* energy storage system at time t in day n [-].
$LoH_{bat,t,n}$	Loss of health of *bat* energy storage system at time t in day n [-].
$Life_{bat}$	Estimated lifetime of *bat* energy storage system [*years*].

I. INTRODUCTION

In recent years, the use of Renewable Energy Sources (RESs) has expanded substantially in both small-scale and large-scale integration. Generated electricity from these abundant sources, such as wind and solar energy, can alleviate many of the issues that power grids are struggling with today. Firstly, by generating electricity inside cities and adjacent to load demand centres, these assets have a huge impact on reducing distribution system network losses. Secondly, by providing a proportion of the increasing electricity demand, they can lower costs for network expansion or postpone it at the very least. While being beneficial to a large extent, the usage of these resources has introduced new challenges. Unlike their conventional fossil-fuel-based rivals, the stochasticity and unpredictability of these sources have introduced new impediments in the energy management of power networks [1]–[3]. The output power of RESs primarily depends on the weather conditions and cannot be accurately predicted [4].

In the last few decades, the technological advancement of Battery Energy Systems (BESs) along with energy conversion systems has made them worthwhile in power grid applications. These units are capable of surmounting numerous current power system issues that come with the utilization of RESs, such as high demand peaks, poor power quality, and voltage fluctuations [5]. As a viable solution to these issues, BES units can be scheduled to charge in off-peak hours and discharge in peak hours, which benefits the system in terms of reducing line congestion as well as operating costs [6]. Frequent usage, however, along with overcharging or overdischarging, does harshly harm their health conditions and leads to a reduction in their lifetime [7], [8]. Thus, an optimal charging schedule and strategy as well as an accurate lifetime model are required to not only reduce grid operation expenses but also result in BES's longer lifespan.

A. LITERATURE REVIEW

In the existing literature, a number of algorithms are used to model BES, which are different in terms of accuracy, speed, and practicability, and each has unique advantages and flaws. Firstly, Peukert Lifetime Energy Throughput (PLET) is one method, which is utilised in [9], where BES sizing and lifetime, as well as grid costs, are the main objectives. This model is also taken into account in [10], [25] with simplifying assumptions, with goals such as optimally operating network and prolonging battery life. However, this method, which measures battery loss of health by the output current in each cycle, was first introduced for small-scale batteries and is not completely appropriate in terms of accuracy for power grid applications. Secondly, the Ampere-hour throughput model is widely considered in the existing literature. In [23], this method is used on a residential network and small-scale units to anticipate the life depreciation of electric vehicle batteries with the objective of prolonging their life and decreasing customers' electricity costs. Compared to other BES lifetime methods, however, this model is less accurate. Therefore, in some research, such as [26] and [27], a modified version of this model with higher precision is used, particularly for Li-ion batteries in BES and wind farm correlation. Additionally, this method is implemented in [28] to anticipate the end of life of Li-ion batteries and assess their economic benefits. Finally, another technique to assess the BES lifetime in various conditions is the Rain-Flow Cycle Counting (RFCC) model. By conducting several laboratory experiments, the RFCC and Ah throughput models are compared in terms of accuracy in [29]. According to this reference, while being more complicated, the RFCC method has the benefit of higher precision, since it considers more stress factors (destructive inherent and ambient elements that a battery faces in its lifespan). In [11], it is used for lead-acid batteries, and the simulation required data is obtained from the manufacturer's

TABLE 1. A comparison taxonomy of the reviewed papers.

Ref.	Active Power Losses	Linearised AC-OPF	Renewable Energy Sources		Battery Technology	Rain-Flow Cycle Counting Method	Battery Linear Lifetime Curve	Uncertain Parameters			Mathematical Modelling	Type of Objective Function
			Solar	Wind				Load	Solar	Wind		
[9]					Li-ion			✓			NLP	Multi
[10]			✓	✓	N/A			✓	✓	✓	NLP	Single
[11]				✓	Lead-Acid	✓				✓	NLP	Multi
[12]				✓	N/A	✓				✓	NLP	Multi
[13]				✓	Li-ion						NLP	Single
[14]				✓	N/A			✓		✓	MILP	Single
[15]	✓				Li-ion	✓					NLP	Single
[16]	✓*				Lead-Acid						MILP	Multi
[17]	✓		✓	✓	Li-ion						LP	Multi
[18]	✓				Li-ion						PSO	Multi
[19]	✓				Lead-Acid						PSO	Multi
[20]	✓			✓	N/A						GA	Multi
[21]	✓				ZnBr						PSO	Single
[22]	✓				N/A						PSO	Single
[23]			✓		Li-ion			✓	✓		MILP	Multi
[24]			✓		Li-ion	✓	✓	✓	✓		MILP	Multi
This paper	✓	✓	✓	✓	Li-ion	✓	✓	✓	✓	✓	MILP	Multi

* A weighted power loss function is used in the objective function.

datasheets. In [24], this method is taken into account in an operational problem with the objective of extending the BES lifetime and lowering operating costs. In this reference, a plain DC-OPF is introduced, which does not consider network losses thoroughly. In [12], [13], with some modifications to the model details, this approach is used for battery life extension to achieve higher accuracy and lower complexity.

Another substantial element that needs to be addressed is future demand and supply predictions, for in real-world conditions, the output power of RESs and day-ahead customer demand are uncertain variables. Stochastic programming is widely used to tackle this issue by considering highly probable scenarios for these variable events in power grids [30]–[33]. A stochastic problem with a two-stage solution with uncertain load demands, PV, and wind generation is taken into account in [34]. In addition, a large number of scenarios (which are highly probable) are considered, and a data clustering method is implemented to reduce their quantity and solve them in two stages. In [10], a neural-network-based stochastic approach is taken into account to anticipate future load demand and PV generation.

B. CONTRIBUTIONS SUMMARY

Based on the reviewed literature and to the authors' best knowledge, a gap exists in the modelling techniques and methods that are utilised in the existing research works. Hence, in this work, an EMS framework with linearised approach and in-depth analysis on BES life extension is presented which optimises the techno-economic aspects of an Active Distribution Network (ADN) connected to BESs and RESs. This includes a dual-objective model to determine the optimum scheduling scheme for BESs both to minimize electricity purchasing costs from the perspective of Distribution System Operators (DSOs) and to maximize the life expectancy of BES units. The novelties in this paper include, but are not limited to, formulating the problem as a stochastic, Mixed-Integer Linear Programming (MILP) model, meaning that all non-linear elements of the problem are linearised using mathematical techniques. Furthermore, a satisfactory, accurate, rapid, and linearised AC power flow method is adopted for the first time in the context of scheduling BESs and distribution EMSs. These qualities in solving energy management problems—accuracy and speed—are of high importance, especially for DSOs to schedule charging/discharging based on the future energy price signal and predicted renewable generation to meet load demand, maximise revenue as well as minimise costs, and shave demand peaks as much as possible. Regarding numerical studies, to illustrate the viability of this methodology, the proposed algorithm is tested on a manipulated radial network. Table 1 presents a taxonomy to highlight the novelties of the present paper compared to previous research. To summarise, the main contributions of this paper are as follows:

1) Developing a two-stage stochastic optimisation framework with the K-means clustering method as the reduction algorithm to tackle the uncertainties associated with the load demand and renewable generations -solar and wind energies- considering historical weather conditions and time of the year for a one-year period.
2) Implementing an epsilon-relaxed linearised AC Optimal Power Flow (OPF) model on a radial network for the first time in the BES scheduling context. In contrast to

previously introduced linear OPFs in the existing literature, this method contains no binary variable. As a result, with relatively high accuracy, it has less execution time, which makes it a suitable choice for implementation in real-world large-scale distribution networks.

3) Implementing a linearised RFCC method for battery life expectancy estimation. Extending existing work, a piecewise linearisation technique is taken into account to formulate the battery life based on its discharge rate. As a whole, by adopting this technique, we developed a MILP formulation, achieving a globally optimal solution which cannot be achieved in a Non-Linear Programming (NLP) solution.

The remainder of this paper is organised as follows: Section II describes the general concept of the proposed model. Section III presents the objective function and formulation of the model. The BES units' lifetime model is explained in Section IV. The chosen stochastic approach is presented in section V. In Section VI, the details of the proposed case study based on a modified 33-bus radial distribution system are depicted, and simulation results are presented. Conclusions are made in Section VII and the future possible developments of this paper are given.

II. MODEL OUTLINE

The general framework of the proposed model is illustrated in Fig. 1. According to this model, BESs are employed as assets to shift loads from peak hours to off-peak ones. To this end, these resources are being controlled by a centralised EMS which determines when they should be connected to the distribution network and when it is more economical to isolate them. It also dictates charging/discharging patterns and rates for BESs when they are connected to the network. These decisions are made based on various variables such as energy prices (provided by the DSO throughout the day), network characteristics and constraints, and the predicted loads of the customers as well as renewable generations. The main goal of the system is to schedule the BESs to not only extend their lifetime but also to decrease the network operating costs as much as possible. While there are a number of studies in the current literature using control algorithms in event-triggered fuzzy as well as neural-network-based event-triggered adaptive methods in [35], [36], this paper focuses on the optimisation approaches in energy management to optimally schedule BESs in an ADN.

Two-stage stochastic programming is engaged to tackle the uncertainty of the problem. Here, renewable generation and load demand are considered as uncertain variables, meaning that they can take different quantities in each scenario. To generate realistic scenarios based on historical data, initial data including wind speed, solar irradiance, and load profile are required, which are extracted from historical real-world databases. Subsequently, based on the inherent characteristics of each data set, an appropriate probability distribution function is chosen, and scenarios are generated accordingly.

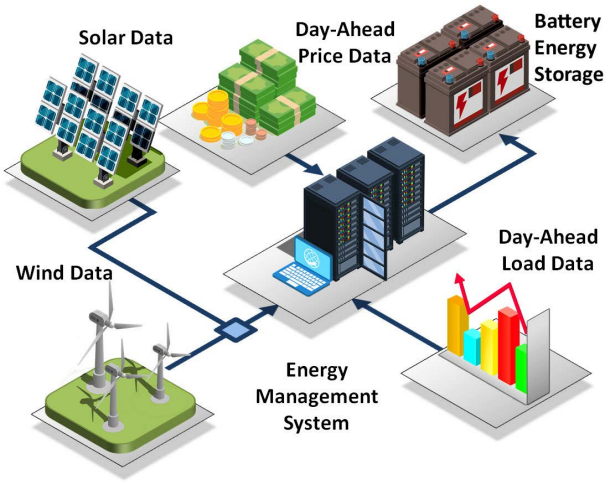

Some of the symbols are taken from freepik.com website.

FIGURE 1. Energy storage system scheduling in the proposed framework.

To manage a large number of scenarios, the K-means clustering method is used to shrink the number of scenarios for calculating first-stage variables. While reducing scenarios occasionally leads to data loss and incorrect density of data in each region, this method retains the distribution of the main scenarios in each region to a great degree, making the output reduced scenario data set more reliable. Finally, by considering the first-stage variables as constants and solving the stochastic problem with the main scenarios, the second-stage variables and their expected values are computed. Fig. 2 illustrates the main algorithm of the proposed model.

Another significant element that needs to be addressed in operational problems is the OPF method. Several existing methods are focused on AC non-linear iterative models [37], [38]. Nevertheless, these methods—while having the advantage of accuracy—are considerably slow in solving time, particularly for large networks. On the other hand, despite having the advantage of high solving speed, the linear DC-OPF method is not always the best option. Since it does not take bus voltages, network losses, and reactive power into account, the results of this solution are not genuinely accurate. To get the best out of both, several linearised AC-OPF methods [14], [39]–[41] were assessed. These are formulated and compared with each other on some criteria, such as calculation speed, accuracy, and compatibility with distribution networks. While some of these methods were more accurate, the solving time and complexity of implementation were burdensome in some cases. The algorithm in [14], which is based on minimal approximations, was chosen to be implemented since it was introduced mainly for distribution networks and is rapid in calculation while having fair precision. Additionally, it results in a globally optimal solution which cannot be obtained by NLP methods. This model was formerly introduced for network reconfiguration.

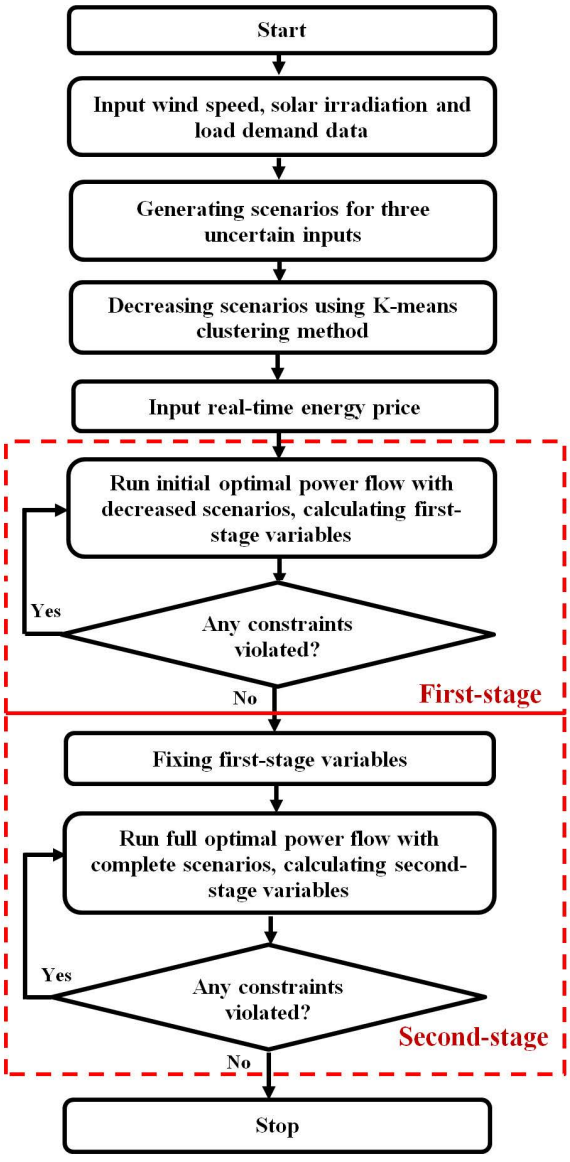

FIGURE 2. Problem solving algorithm.

III. PROBLEM FORMULATION

In this paper, we undertake a MILP formulation to solve the proposed problem. The main goal is to calculate the optimal charging/discharging power as well as its pattern throughout the day such that it can bring the minimum cost to the DSO while maximizing the life span of BESs. Later in this section, different aspects of the formulation, including objective function, network constraints, cost-based formulas, and the linear AC-OPF model, are explained.

A. OBJECTIVE FUNCTION

In the proposed bi-objective problem, the operating cost of the system is considered as the main objective. This includes the cost of energy purchased from the upstream network by the DSO. The second objective is the lifetime of BESs, which here is converted to a price-based term to match the unit of the main objective. The complete objective function is defined by (1) which is a cost-based equation and is required to be minimised in the optimisation problem.

$$min\ OF = \sum_{\omega\in\Omega^{\omega}}^{n} p_{\omega}\left[Cost_{\omega}^{Net} + Cost^{BES}\right] \tag{1}$$

It should be noted that since we introduced stochastic programming, second-stage cost terms take scenario indices. Nonetheless, $Cost^{BES}$ (as a first-stage variable) is calculated with decreased scenarios and appears as fixed in the second-stage calculation, and therefore, it does not take a scenario index. The operating cost of each scenario is multiplied by its chance of occurrence, and finally, the expected cost of operation is calculated as the ultimate objective function. Network costs are explained in the next subsection, and $Cost^{BES}$ is comprehensively explained in section IV.

B. GRID COSTS AND BES CONSTRAINTS

The upstream network cost equations are shown in (2),where the electricity unit price, $Price_{i,t}$, is considered as a constant parameter. Other constraints regarding BES modelling are shown in (3)-(6). Equation (3) is the operating constraint which calculates the SoC of each BES throughout the day based on its initial, input, and output energy. Equation (4)-(6) are inequalities regarding battery charging and discharging limits and battery high and low energy limits.

$$Cost_{\omega}^{Net} = \sum_{t\in\Omega^{t}}\sum_{i\in\Omega^{B}} P_{i,t,\omega}^{G}\,\Delta t\,Price_{i,t} \quad \forall\omega\in\Omega^{\omega} \tag{2}$$

$$SoC_{bat,t} = SoC_{bat,t-1} + \eta^{ch}P_{bat,t}^{ch}\Delta t - \frac{1}{\eta^{dch}}P_{bat,t}^{dch}\Delta t \quad \forall bat\in\Omega^{bat},\quad \forall t\in\Omega^{T} \tag{3}$$

$$0 \le P_{i,t}^{dch} \le \overline{P^{dch}} \quad \forall i\in\Omega^{B},\ \forall t\in\Omega^{T} \tag{4}$$

$$0 \le P_{i,t}^{ch} \le \overline{P^{ch}} \quad \forall i\in\Omega^{B},\ \forall t\in\Omega^{T} \tag{5}$$

$$\underline{SoC} \le SoC_{bat,t} \le \overline{SoC} \quad \forall bat\in\Omega^{bat},\ \forall t\in\Omega^{T} \tag{6}$$

C. LINEARISED AC-OPF

In this work, the OPF problem is formulated as a linearised AC-OPF model, which was previously introduced in [14]. Nonetheless, we implemented this formulation for BES scheduling for the first time. All equations associated with the proposed network model are shown as (7)-(18). Equation (7) and (8) are related to supply and demand balancing considering renewable generations for active and reactive power, respectively. Equation (9) calculates bus voltages, (10) and (11) are inequalities associated with maximum and minimum limits of voltages, and (12) specifies the current limit of network lines. Equation (13)-(15) and (16)-(18) are two sets of linear equalities and inequalities that linearise the expression $P^2 + Q^2 = S^2$. These equations are thoroughly explained in [14] and in [42]. It is worth mentioning that λ,

the piecewise linearisation parameter for OPF, is set to 6.

$$P^{G}_{i,t,\omega} + P^{Wind}_{i,t,\omega} + P^{PV}_{i,t,\omega} + \sum_{ki\in\Omega^{L}} \left[P_{ki,t,\omega} - R_{ki} f_{ki,t,\omega}\right] - \sum_{ij\in\Omega^{L}} P_{ij,t,\omega} - \left(P^{ch}_{bat,t} - P^{dch}_{bat,t}\right) = P^{Load}_{i,t,\omega}$$
$$\forall bat \in \Omega^{bat}, \forall \omega \in \Omega^{\omega}, \quad \forall i \in \Omega^{B}, \ \forall t \in \Omega^{T} \quad (7)$$

$$Q^{G}_{i,\omega} + \sum_{ki\in\Omega^{L}} \left[Q_{ki,t,\omega} - X_{ki} f_{ki,t,\omega}\right] - \sum_{ij\in\Omega^{L}} Q_{ij,t,\omega} = Q^{Load}_{i,t,\omega}$$
$$\forall \omega \in \Omega^{\omega}, \quad \forall i \in \Omega^{B}, \ \forall t \in \Omega^{T} \quad (8)$$

$$u_{i,t,\omega} - u_{j,t,\omega} = 2\left(R_{ij}P_{ij,t,\omega} + X_{ij}Q_{ij,t,\omega}\right) - \left(Z_{ij}\right)^{2} f_{ij,t,\omega} + \Delta V_{ij,t,\omega}$$
$$\forall \omega \in \Omega^{\omega}, \forall ij \in \Omega^{L}, \forall t \in \Omega^{T} \quad (9)$$

$$\left(\underline{V}\right)^{2} \le u_{i,t,\omega} \le \left(\overline{V}\right)^{2} \quad \forall \omega \in \Omega^{\omega}, \ \forall i \in \Omega^{B}, \ \forall t \in \Omega^{T} \quad (10)$$

$$\left|\Delta V_{i,t,\omega}\right| \le \left(\overline{V} - \underline{V}\right)\left(1 - q_{ij,t,\omega}\right)$$
$$\forall \omega \in \Omega^{\omega}, \quad \forall ij \in \Omega^{L}, \ \forall t \in \Omega^{T} \quad (11)$$

$$0 \le f_{ij,t,\omega} \le \left(\overline{I}\right)^{2} w_{ij,t} \quad \forall \omega \in \Omega^{\omega}, \ \forall ij \in \Omega^{L}, \ \forall t \in \Omega^{T} \quad (12)$$

$$\eta_{l} \ge \left|Q_{ij,t,\omega}\right|, \quad \xi_{l} \ge \left|P_{ij,t,\omega}\right|$$
$$\forall \omega \in \Omega^{\omega}, \quad \forall ij \in \Omega^{L}, \ \forall t \in \Omega^{T}, \forall l = 1 \quad (13)$$

$$\begin{cases} \xi_{l} = \xi_{l-1}\cos\left(\frac{\pi}{2^{l+1}}\right) + \eta_{l-1}\sin\left(\frac{\pi}{2^{l+1}}\right) \\ \xi_{l} = \xi_{l-1}\cos\left(\frac{\pi}{2^{l+1}}\right) + \eta_{l-1}\sin\left(\frac{\pi}{2^{l+1}}\right) \end{cases} \quad \forall l = 2, \ldots, \lambda \quad (14)$$

$$\xi_{l} \le S_{ij,t,\omega} \quad \eta_{l} \le \xi_{l}\tan\left(\frac{\pi}{2^{l+1}}\right)$$
$$\forall \omega \in \Omega^{\omega}, \forall ij \in \Omega^{L}, \forall t \in \Omega^{T}, \forall l = (\lambda + 1) \quad (15)$$

$$\eta_{l} \ge \left|S_{ij,t,\omega}\right|, \xi_{l} \ge \left|\left(u_{i,t,\omega} - f_{ij,t,\omega}\right)/2\right|$$
$$\forall \omega \in \Omega^{\omega}, \forall ij \in \Omega^{L}, \forall t \in \Omega^{T}, \forall l = 1 \quad (16)$$

$$\begin{cases} \xi_{l} = \xi_{l-1}\cos\left(\frac{\pi}{2^{l+1}}\right) + \eta_{l-1}\sin\left(\frac{\pi}{2^{l+1}}\right) \\ \xi_{l} = \xi_{l-1}\cos\left(\frac{\pi}{2^{l+1}}\right) + \eta_{l-1}\sin\left(\frac{\pi}{2^{l+1}}\right) \end{cases} \quad \forall l = 2, \ldots, \lambda \quad (17)$$

$$\xi_{l} \le \left(u_{i,t,\omega} + f_{ij,t,\omega}\right)/2, \quad \eta_{l} \le \xi_{l}\tan\left(\frac{\pi}{2^{l+1}}\right)$$
$$\forall \omega \in \Omega^{\omega}, \quad \forall ij \in \Omega^{L}, \ \forall t \in \Omega^{T}, \ \forall l = (\lambda + 1) \quad (18)$$

IV. BATTERY MODELLING

Generally, a battery's life expectancy is dependent on the number of times it has been charged (or discharged) in its lifetime. Apart from that, the RFCC method implies that the lifetime of a chemical-based battery is dependent on other stress factors, including, but not limited to, the total capacity of the battery, the number of incomplete cycles, the battery's discharging current, temperature, and charging method. The more stress factors are considered, the greater the accuracy of the model will be. Here, it is assumed that the battery ambient temperature is fixed at 25 degrees Celsius. With fair approximation, several stress factors, such as battery capacity, number of discharging cycles, discharging power, and rate of discharge, are taken into account. Less energy exchange between a BES and the connected network can lead to its longer life span. Additionally, the lifetime is also dependent on other factors such as usage patterns, meaning that during a significant rate of charge/discharge in a given time interval, the battery's state of health degrades at a quicker pace. As a consequence, life expectancy is affected more severely. As a solution, if a high-capacity BES is available, the energy could be exchanged in a gradual and steady manner, which results in higher efficiency and a longer BES lifespan.

To follow the life depreciation of BESs, a battery life estimation model based on [29] is introduced. In this process, battery life depreciation is measured by using the cycle-to-failure versus Depth of Discharge (DoD) curve. Fig. 3a portrays an example Li-ion battery lifetime curve which is employed in this work [43]. The RFCC algorithm, which was originally introduced to track material fatigue, is implemented to assess each cycle's effect on the BES lifetime [44].

This battery life assessment algorithm assumes that if the mentioned lifetime curve for DoD of k shows N cycle-to-failure, the storage unit can charge or discharge N times before the end of its life. As a result, if the battery undergoes a cycle with a DoD of k, $1/N$ of its life is lost, and $(N-1)/N$, which we call the remaining life fraction, is the fraction that represents the remaining battery life. As this process continues, when the remaining life fraction reaches zero, the battery is considered to stop operating and this stage is regarded as the battery's end of life. Formerly, the RFCC technique has been successfully implemented for battery lifetime modelling in [11], [12], [29], [45].

To include any fractional charge cycles (which were not available in the manufacturer's datasheet) and their impact on battery life expectancy, the mentioned lifetime curve was extrapolated using a two-term exponential curve fitting equation. The formula and the results of the calculation are shown in (19), and Fig. 3a illustrates the extrapolated curve.

$$C_{f} = A\, e^{B(DoD)} + C\, e^{D(DoD)}$$
$$A = 166100, \ B = -11.11, \ C = 15530, \ D = -1.3 \quad (19)$$

The BES life depreciation in each time interval can be calculated by a piecewise linearised equation which is shown in (20). This linearisation of the cycle-to-failure versus DoD

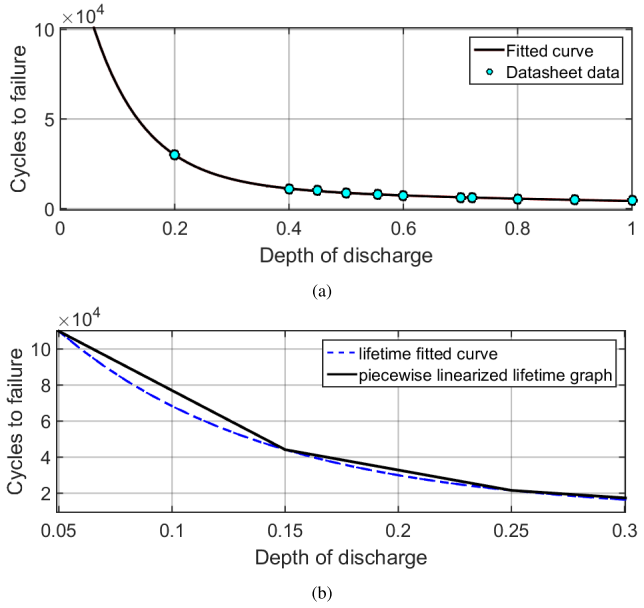

FIGURE 3. (a) Battery lifetime data and extrapolated curve which is used in this paper [43]. (b) linearised lifetime curve for the selected battery to be utilised in a MILP formulation.

curve is undertaken based on battery manufacturer data. Fig. 3b depicts the original and linearised curve. It is worth mentioning that in (20), X_i and Y_i are the horizontal and vertical axis data of the cycle-to-failure versus DoD curve. X_1 and Y_1 are the starting points, and X_2 and Y_2 are the ending points of each section, while X_0 is the predetermined linearisation step (which is assumed to be 5%). Additionally, each BES life expectancy, as well as the deterioration cost of all of these units, are calculated using (21) and (22), respectively.

$$LoH_{bat,t,n} = \left\{ \frac{\frac{1}{Y_2} - \frac{1}{Y_1}}{X_2 - X_1} \left(DoD_{bat,t,n} - X_1 \right) + \frac{1}{Y_1} \mid X_2 = X_1 + X_0 \,,\; X_1 \le DoD_{bat,t,n} \le X_2 \right\} \quad \forall bat \in \Omega^{bat}, \forall t \in \Omega^{t}, \forall n \in \Omega^{year}, \forall X \in \Lambda^{DoD}, \forall Y \in \Lambda^{CtoF} \tag{20}$$

$$Life_{bat} = \frac{1}{\sum_{n \in \Omega^{year}} \sum_{t \in \Omega^{t}} LoH_{bat,t,n}} \quad \forall bat \in \Omega^{bat} \tag{21}$$

$$Cost^{BES} = \sum_{n \in \Omega^{year}} \sum_{t \in \Omega^{t}} \sum_{bat \in \Omega^{bat}} LoH_{bat,t,n} C^{BES}_{bat} \tag{22}$$

V. STOCHASTIC PROGRAMMING

Due to the uncertain nature of input variables—load demand, PV, and wind generation—a two-stage stochastic method is proposed to tackle the uncertainty and fluctuation of these variables. Naturally, more generated scenarios can lead to a more reliable and also more accurate answer. However, considering all possible scenarios can add to the problem's size and complexity, and a trade-off between accuracy and solving speed should be considered.

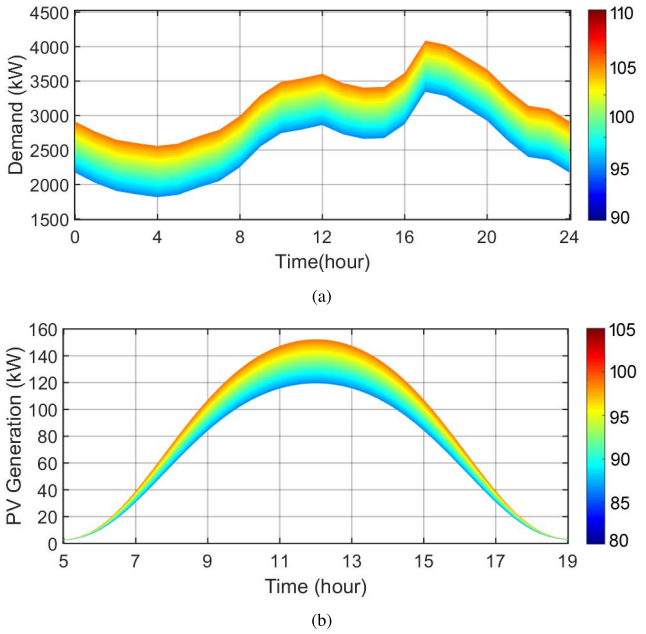

FIGURE 4. (a) Probable load demand area for scenario generation under Gaussian distribution function. (b) Probable photovoltaic generation area in June 1st in the summer for Málaga, Spain based on the historical irradiation data for scenario generation under Beta distribution function [46].

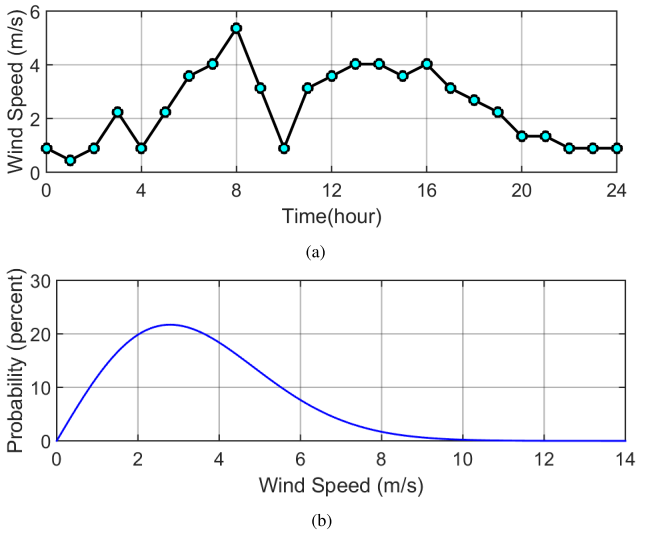

FIGURE 5. (a) Wind speed data of June 1st representing the summer season [47]. (b) wind speed probability based on Rayleigh PDF for 9:00 in June 1st for Málaga, Spain [47].

In terms of load demand uncertainty, 100 scenarios are generated based on a Gaussian Distribution Function (GDF). In each time interval, the maximum deviation of 10% of the maximum daily load is considered. The extra load in each scenario—positive or negative—is randomly distributed to buses that contain load demands. In Fig. 4a, the bounded area for scenario generation of load demands is characterised by the coloured surface.

As for the PV generation stochasticity, the Beta Distribution Function (BDF) is implemented based on the solar irradiance data available in online databases [46]. According to [48], compared to other distribution functions for PV generation outputs, this function results in more accurate and realistic scenarios. A total of 10 scenarios are generated for each time interval, in which every single one deviates from 80% to 105% of the mean value. The coloured surface in Fig. 4b indicates the scenario generation domain.

Lastly, the Rayleigh Distribution Function (RDF), with a fixed shape parameter k set to 2, is engaged to take wind stochasticity into account. This function is a single-parameter one, which can be used for generating accurate wind scenarios [49]. The scale parameter and an RDF scenario generation formula are depicted in (23) and (24), respectively [50].

$$c = \sqrt{\frac{2}{\pi}} v_m \tag{23}$$

$$f(v) = \left(\frac{v}{c^2}\right) e^{-\frac{v^2}{2c^2}} \tag{24}$$

where c is the scale parameter, v and v_m are wind speed and mean wind speed, respectively. In total, 10 random scenarios are generated based on the historical wind speed data for each time interval. Fig. 5a illustrates wind speed captured on the first day of summer in 2019, based on historical data [47]. Fig. 5b shows an example of wind speed probability based on Rayleigh PDF at 9:00 on the same day with an average wind speed of 3.7 m/s. The scenarios are generated according to the probability distribution of this curve for the mentioned date and time and likewise for other time intervals.

The results are calculated by taking each of the 100 load scenarios and each of the 10 renewable scenarios. As a result, for each time interval, $10 \times 100 = 1000$ scenarios are generated. In total, this will leave us with a 1000×24 scenario matrix. A large number of scenarios lead to a complicated problem, and usually it is shrunk to a sensible one with the same range and distribution density as the original scenarios. Cluster analysis has been used in many existing research works to separate items from a set with similar inherent specifications. In this paper, the K-means clustering method as a type of cluster analysis is employed to shrink the number of scenarios, since it has been widely used and tested successfully in previous research [34], [51], [52]. After generating the main scenarios, a single-dimensional K-means clustering method is employed to reduce the number of scenarios to 10 for each time interval, resulting in 10×24 scenario matrix.

In this paper, control variables in the proposed model are divided into two groups. First-stage variables are $P^{ch}_{bat,t}$ and $P^{dch}_{bat,t}$, which are calculated on the first program running considering a reduced number of scenarios. After the first stage of simulation, these variables are fixed and treated as constants. Subsequently, the problem is solved using the original scenarios and second-stage variables consisting of $V_{i,t,\omega}$, $I_{ij,t,\omega}$, $P_{ij,t,\omega}$, $Q_{ij,t,\omega}$, and other variables with index ω. The expected value of OF is calculated using the mathematical expressions explained in the previous section and the probability of each scenario.

TABLE 2. Specifications of energy storage systems.

Parameter	Notation	Value	Unit
BES type	-	Li-ion	-
Unit price		150	\$/kWh
Maximum power of each unit		100.8	kWh
Cost of each unit	C^{BES}_{bat}	15120	\$
Charging efficiency	η^{ch}	95	%
Discharging efficiency	η^{dch}	95	%
Maximum charging rate	$P^{ch}_{bat,t}$	50	%/hour
Maximum discharging rate	$P^{dch}_{bat,t}$	50	%/hour
Maximum state of charge	$\overline{SoC}$	100	%
Minimum state of charge	$\underline{SoC}$	10	%
Initial state of charge	-	10	%

VI. SIMULATION AND RESULTS

A. CASE STUDY

In the present paper, a modified radial distribution network (20.9 kV) with 33 buses is considered to be used as a test system. The original network data for the simulation were obtained from [53]. The assumed test system along with the added components is depicted in Fig. 6. It is worth mentioning that RESs are considered non-dispatchable and their generated power is consumed as it is produced.

In terms of load demand, a seasonal load profile is considered, which takes four separate curves for each season into account. To reduce the size of demand data, the first day of each season is assumed to represent the entire season. Therefore, four different load profiles for Málaga, Spain (the chosen site for our network) are obtained from [54], which are illustrated in Fig. 7. In scenarios in which the load demands are higher or lower than the original network [53], the excess load demand is distributed to the buses proportionally (based on their original load).

The electricity price is assumed to follow a market-based RTP scheme. In this paper, two representative curves for the entire year are considered to reduce the bulky data input, one representing spring and summer, and the other representing autumn and winter. The prices for the first day of summer and winter are assumed to represent the warm and cold seasons, respectively. These figures and data are taken from [55], which are illustrated in Fig. 8.

According to [43], each battery pack with a 110Ah capacity can store approximately 1.4kWh. In our proposed network, each BES unit includes 72 battery packs, which raises the total capacity to 100.8 kWh. According to [56], in the simulation period, the BES system investment cost is presumed to be \$150/kWh. The data for BES units are depicted in Table 2.

Concerning renewable generation, each PV unit's maximum generation is set at 50 kW (see Fig. 4b). The generated power is based on solar irradiance data obtained from [46]. In addition, each wind unit's capacity is nominally 100 kW. The wind speed data at 10 meters above ground are obtained

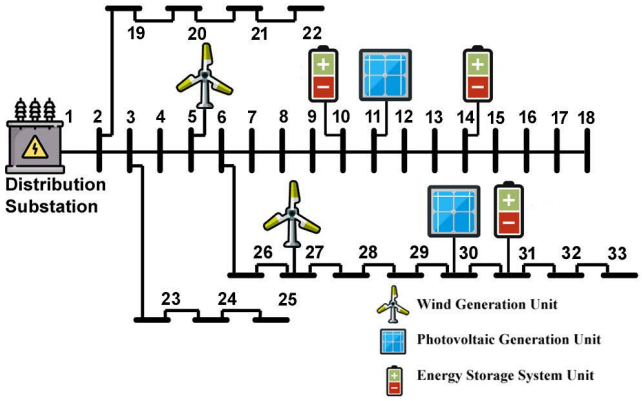

Some of the symbols are taken from freepik.com website.

FIGURE 6. Modified 33-bus distribution test network [53].

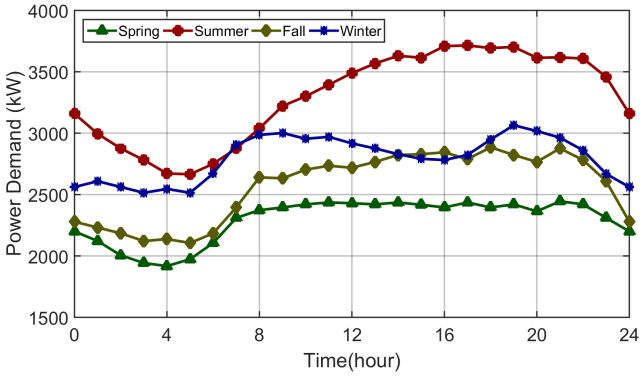

FIGURE 7. Representative load profiles for each season.

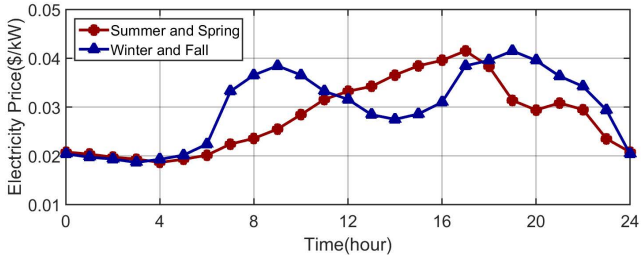

FIGURE 8. Representative network prices for cold (autumn and winter) and warm seasons (spring and summer).

from [47], and the power is calculated proportionally. It is worth mentioning that, similar to load demand data, for renewable generations, the first day of each season is assumed to represent the entire season. The renewable site is considered to be in Málaga, Spain, which is located at coordinates of 36.71 degrees North and 4.41 degrees West.

The processor for the simulation platform is Intel(R) core-i5 @ 2.30GHz and 4GB of RAM. Scenarios generation and graph linearisation are conducted with MATLAB software. The optimisation problem is solved using GAMS software with the CPLEX linear solver.

TABLE 3. Numerical results of the three assumed cases in a one-year simulation period.

Results	Simulation cases			Unit
	Case A	Case B	Case C	
Spring operating cost	133786.5	134135.7	133715.5	$/season
Summer operating cost	207085.9	207402.9	206995	$/season
Autumn operating cost	171227	171997.5	171113.5	$/season
Winter operating cost	182171	182875.9	182062.4	$/season
Total operating cost	694270.4	696412	693886.4	$/year
Upstream Network cost	694270.4	692043.4	691805.8	$/year
BES operating cost	-	4368.6	2080.6	$/year
BES life expectancy	-	10.4	21.8	year

Regarding the evaluation of the results, the problem is solved in three different cases. These cases are defined as follows:

Case A: BES units are not considered.
Case B: BES units are considered but the lifetime model is not employed.
Case C: BES units are considered and the lifetime model is employed.

B. NUMERICAL RESULTS

The proposed optimisation problem is solved based on the data assumed in the previous subsection. As for the numerical results, expected costs are calculated for four representative days of each season and generalised to that whole season for each case. Finally, by adding these numbers together, the expected cost for a year is calculated. The numerical results for the case studies are shown in Table 3.

In case A, only the effects of RESs are considered, removing BESs from the network. According to the data depicted in Table 3, in this case, the operating cost of the system is relatively high.

In case B, while considering BES units, no lifetime algorithm is implemented, meaning that $Cost^{BES}$ is removed from the objective function equation (see section III). Even though BESs are charged in off-peak hours (when the electricity price is lower) and discharged in peak hours when the electricity price is higher, it is observed that the cost of the operation increases in each season and in total, in comparison to case A. As a result, the expected operating cost is 0.31% higher than that of case A. This mainly happens because the BES units are employed fully without any consideration, and the LoH of each unit is significantly high during charge/discharge cycles.

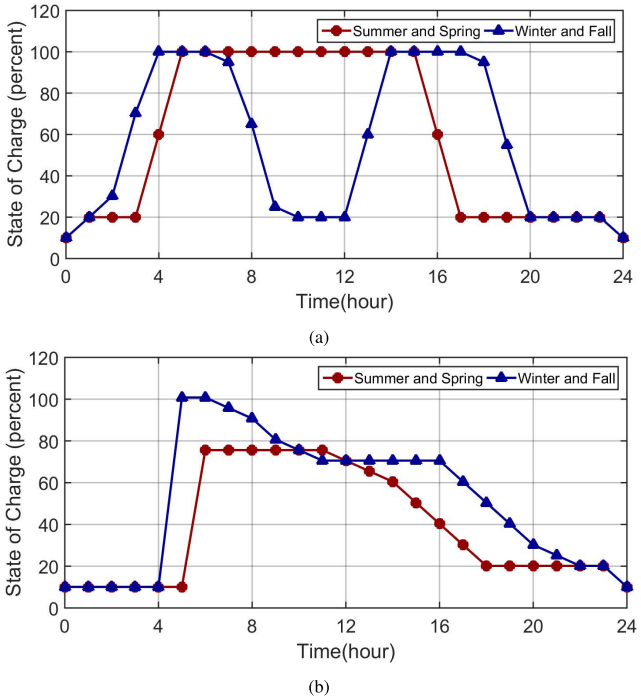

FIGURE 9. (a) State of charge in percentage in case B in each day (b) State of charge in percentage in case C in each day.

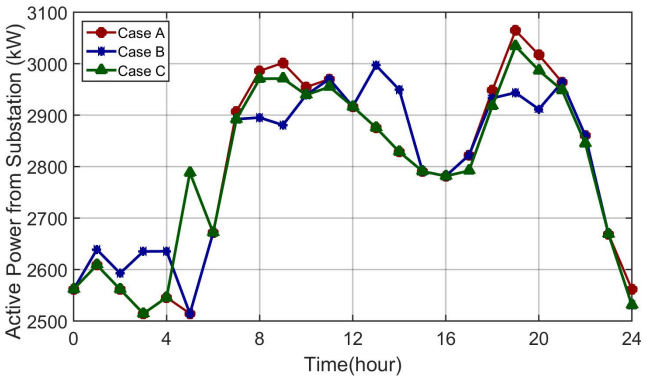

FIGURE 10. Peak shaving assessment for each case in winter load profile.

TABLE 4. Comparison of the accuracy and speed of three algorithms.

Results	Solving Algorithm		
	DC-OPF	Linearised AC-OPF (used in this paper)	AC-OPF
Objective function($)	2267.81	2483.06	2508.22
Solving time(sec.)	0.418	4.088	30.250
Solution status	Globally optimal	Globally optimal	Locally optimal

In other words, the entire capacity of the BES is employed, which influences their lifespan in a negative and destructive manner. Furthermore, these units discharge at a tremendous rate, and their minimum rate is as high as $C/3$ which influences BES lifetime. Fig. 9a illustrates each BES's SoC in warm and cold seasons in case B.

Finally, for case C, the code is compiled and run with the same BESs, while considering the life expectancy of these units and including it in the objective function. In contrast, the operating costs are lower than in previous cases. Generally, the expected operating cost is 0.05% and 0.36% lower than in cases A and B, respectively. Based on the equations, in this last case simulation, the objective goals are achieved by utilising BESs in a moderate and intelligent manner, which results in not only reducing the total expected cost but also their lifetime extension. In Fig. 9b, the charging pattern of each BES unit in case C is illustrated for the warm and cold seasons, respectively. The curves show that in case C, each BES unit has a lower discharging rate compared to case B, which at most is less than $C/8$. In cold seasons, as two price peaks exist in the price curve, they are charged fully. However, in warm seasons with one electricity price peak, they are only charged up to 81% of their capacity. As a result, the deterioration cost of BESs is relatively lower.

The results indicate that the life expectancy of BESs rises significantly from 10.4 years in case B to 21.8 years in case C, an increase of approximately 110%. This numerical assessment demonstrates that a lower discharge rate and scheduled utilisation can extend the BES lifetime considerably, as can be seen by comparing Fig. 9a and Fig. 9b for cases B and C.

C. PEAK SHAVING ASSESSMENT

In this subsection, the effect of using BESs on network load flattening is demonstrated. The winter season load profile was chosen to analyse the data, as unlike other seasons, it has two distinguishing peaks and valleys, which allows one to compare the data more comprehensively. The load demand from the upstream network throughout the day for the winter season is depicted in Fig. 10 for three assumed cases. In case A, no BES is considered; RESs account for a slight demand reduction. According to the graph, uncoordinated usage of BESs in case B allows load shifting to happen in a relatively high and radical manner, and therefore the maximum demand supplied by the upstream network decreases approximately by 2.3% to be 2996 kW. In case C, however, the discharge rate is limited, and consequently, the proposed lifetime model accounts for only a 1% reduction in the maximum network demand, which will be 3034 kW.

D. COMPUTATIONAL TIME AND ACCURACY

To evaluate the model in terms of accuracy and solving time, two other common power flow algorithms, DC-OPF and AC-OPF, have been developed to solve the existing problem. The models are standard linear DC-OPF approximations (without considering reactive power and voltage angle) and a Newton-Raphson based AC-OPF obtained from [57]. This allows for a comparison of the undertaken linearised AC-OPF

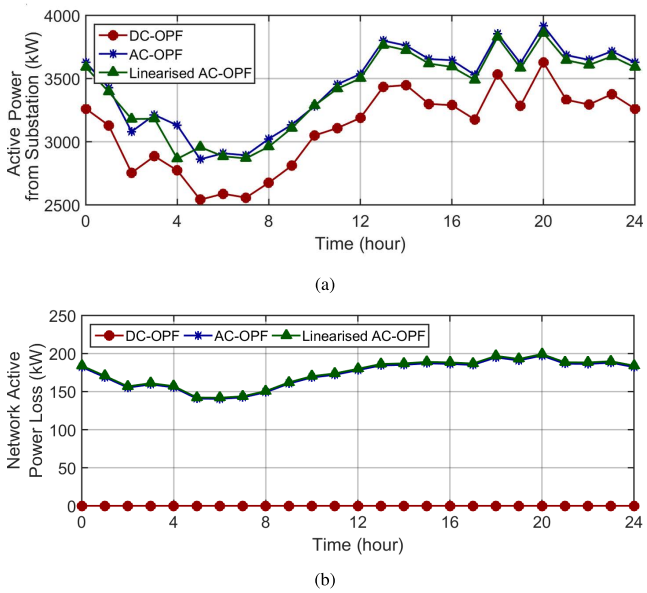

FIGURE 11. (a) The power injected to the power grid from substation in three assessed optimal power flow algorithms. (b) The active power loss of the three assessed optimal power flow algorithms.

with other methods used in existing research. In formulating the other two OPF methods, (1)-(6) and (19)-(24) (which are equations regarding basic constraints and battery as well as stochastic modelling) were unchanged, and the remaining equations were replaced with the main algorithms of the new methods.

The solving time, objective function quantity, and the solution status for solving one scenario under three different algorithms are demonstrated in Table 4. According to these data, with relatively high accuracy compared to the DC-OPF method and approximately 90% less error, the linearised AC-OPF model significantly increases the calculation speed compared to the original AC-OPF model (nearly 7 times faster), while calculating a globally optimal solution. In Fig. 11, $P^{G}_{i,t,\omega}$ or the power absorbed from the substation as well as total active power loss of the network are depicted for three mentioned power flow algorithms. It can be observed that while in the DC-OPF the power loss is zero and the total power from the substation is the least, in linearised AC-OPF algorithm the power loss and power absorbed from the substation is slightly less than in the original AC-OPF method in most time intervals.

VII. CONCLUSION

In this paper, a BES scheduling problem in an ADN is proposed. Operating cost minimization as well as BES lifetime extension are set as the main objectives of the problem. In terms of considering uncertainty, a two-stage stochastic optimisation approach is implemented, and K-means clustering as a scenario number reduction method is engaged. As for the core operation problem, a linearised, convexed AC-OPF model with high calculating speed and fair accuracy is put into practice. Finally, a linearised method based on the RFCC technique is implemented to track BES's deterioration and evaluate the LoH of the battery during the simulation period.

The simulation results indicate that:

- Considering the lifetime model, BESs are discharged moderately, while without the lifetime model, they are discharged at a substantial rate and fully charged several times a day.
- The operating cost is highest when using BESs without the lifetime model and lowest when optimally scheduling them.
- The life expectancy of BESs is extended by 110% by using the proposed scheduling model.
- The peak demand is reduced by more than 1% in peak hours, which can be decreased further with higher BES capacity.
- By employing the linearised AC-OPF, the execution time is reduced significantly (nearly 85%) compared to the original non-linear formulation, while guaranteeing fair accuracy (approximately 1% error in the objective function).

In future work, some modifications can be made to the proposed model to enhance it in terms of accuracy. First, we only assessed Li-ion batteries in this work. By working on different battery types on the same network, the results can be compared in terms of battery life expectancy and grid profit. Second, in this paper, it is assumed that the price of BES units would remain constant throughout the operating period. However, as time passes, by introducing new technologies and methods of manufacturing, they become less expensive. As a result, by implementing an interest rate, their price decrease in the operating period can be taken into account.

REFERENCES

[1] R. Sharifi, S. H. Fathi, and V. Vahidinasab, "Customer baseline load models for residential sector in a smart-grid environment," *Energy Rep.*, vol. 2, pp. 74–81, Nov. 2016.
[2] Y. Li and J. Wu, "Optimum integration of solar energy with battery energy storage systems," *IEEE Trans. Eng. Manag.*, vol. 69, no. 3, pp. 697–707, Jun. 2022.
[3] P. H. Divshali, B. J. Choi, and H. Liang, "Multi-agent transactive energy management system considering high levels of renewable energy source and electric vehicles," *IET Gener., Transmiss. Distrib.*, vol. 11, no. 15, pp. 3713–3721, 2017.
[4] H. Bevrani, M. R. Feizi, and S. Ataee, "Robust frequency control in an islanded microgrid: H_∞ and μ-synthesis approaches," *IEEE Trans. Smart Grid*, vol. 7, no. 2, pp. 706–717, Mar. 2016.
[5] N. T. Mbungu, R. M. Naidoo, R. C. Bansal, and V. Vahidinasab, "Overview of the optimal smart energy coordination for microgrid applications," *IEEE Access*, vol. 7, pp. 163063–163084, 2019.
[6] M. Alimardani and M. Narimani, "A new energy storage system configuration to extend Li-ion battery lifetime for a household," *IEEE Can. J. Electr. Comput. Eng.*, vol. 44, no. 2, pp. 171–178, Spring 2021.
[7] I. Hauer, S. Balischewski, and C. Ziegler, "Design and operation strategy for multi-use application of battery energy storage in wind farms," *J. Energy Storage*, vol. 31, Oct. 2020, Art. no. 101572.
[8] N. G. Cobos, J. M. Arroyo, N. Alguacil, and J. Wang, "Robust energy and reserve scheduling considering bulk energy storage units and wind uncertainty," *IEEE Trans. Power Syst.*, vol. 33, no. 5, pp. 5206–5216, Sep. 2018.

[9] D. Tran and A. M. Khambadkone, "Energy management for lifetime extension of energy storage system in micro-grid applications," *IEEE Trans. Smart Grid*, vol. 4, no. 3, pp. 1289–1296, Sep. 2013.

[10] Y. Qin, H. Hua, and J. Cao, "Stochastic optimal control scheme for battery lifetime extension in islanded microgrid via a novel modeling approach," *IEEE Trans. Smart Grid*, vol. 10, no. 4, pp. 4467–4475, Jul. 2019.

[11] A. M. Gee, F. V. P. Robinson, and R. W. Dunn, "Analysis of battery lifetime extension in a small-scale wind-energy system using supercapacitors," *IEEE Trans. Energy Convers.*, vol. 28, no. 1, pp. 24–33, Mar. 2013.

[12] X. Ke, N. Lu, and C. Jin, "Control and size energy storage systems for managing energy imbalance of variable generation resources," *IEEE Trans. Sustain. Energy*, vol. 6, no. 1, pp. 70–78, Jan. 2015.

[13] D.-I. Stroe, V. Knap, M. Swierczynski, A.-I. Stroe, and R. Teodorescu, "Operation of a grid-connected lithium-ion battery energy storage system for primary frequency regulation: A battery lifetime perspective," *IEEE Trans. Ind. Appl.*, vol. 53, no. 1, pp. 430–438, Jan./Feb. 2017.

[14] A. Kavousi-Fard, A. Zare, and A. Khodaei, "Effective dynamic scheduling of reconfigurable microgrids," *IEEE Trans. Power Syst.*, vol. 33, no. 5, pp. 5519–5530, Sep. 2018.

[15] B. Xu, A. Oudalov, A. Ulbig, G. Andersson, and D. S. Kirschen, "Modeling of lithium-ion battery degradation for cell life assessment," *IEEE Trans. Smart Grid*, vol. 9, no. 2, pp. 1131–1140, Mar. 2018.

[16] X. F. Dong, Y. Y. Zhang, and T. Jiang, "Planning-operation co-optimization model of active distribution network with energy storage considering the lifetime of batteries," *IEEE Access*, vol. 6, pp. 59822–59832, 2018.

[17] S. Torre, J. M. González-González, J. A. Aguado, and S. Martín, "Optimal battery sizing considering degradation for renewable energy integration," *IET Renew. Power Gener.*, vol. 13, no. 4, pp. 572–577, Mar. 2019.

[18] K. Liu, C. Zou, K. Li, and T. Wik, "Charging pattern optimization for lithium-ion batteries with an electrothermal-aging model," *IEEE Trans. Ind. Informat.*, vol. 14, no. 12, pp. 5463–5474, Dec. 2018.

[19] Y. Zheng, Z. Y. Dong, F. J. Luo, K. Meng, J. Qiu, and K. P. Wong, "Optimal allocation of energy storage system for risk mitigation of DISCOs with high renewable penetrations," *IEEE Trans. Power Syst.*, vol. 29, no. 1, pp. 212–220, Jan. 2014.

[20] S. Koopmann, M. Scheufen, and A. Schnettler, "Integration of stationary and transportable storage systems into multi-stage expansion planning of active distribution grids," in *Proc. IEEE PES ISGT Eur.*, Oct. 2013, pp. 1–5.

[21] M. Sedghi, M. Aliakbar-Golkar, and M.-R. Haghifam, "Distribution network expansion considering distributed generation and storage units using modified PSO algorithm," *Int. J. Electr. Power Energy Syst.*, vol. 52, pp. 221–230, Nov. 2013.

[22] H. Saboori, R. Hemmati, and V. Abbasi, "Multistage distribution network expansion planning considering the emerging energy storage systems," *Energy Convers. Manage.*, vol. 105, pp. 938–945, Nov. 2015.

[23] A. Soleimani, V. Vahidinasab, and J. Aghaei, "Enabling vehicle-to-grid and grid-to-vehicle transactions via a robust home energy management system by considering battery aging," in *Proc. Int. Conf. Smart Energy Syst. Technol. (SEST)*, Sep. 2021, pp. 1–6.

[24] A. Soleimani and V. Vahidinasab, "Integrating battery condition and aging into the energy management of an active distribution network," in *Proc. Smart Grid Conf. (SGC)*, Dec. 2019, pp. 1–6.

[25] H. M. Shin, S.-H. Park, J. Jung, S. Lee, and I. Lee, "Maximization of total throughput and device lifetime with non-linear battery properties," *IEEE Trans. Wireless Commun.*, vol. 16, no. 12, pp. 7774–7784, Dec. 2017.

[26] J. Wang, P. Liu, J. Hicks-Garner, E. Sherman, S. Soukiazian, M. Verbrugge, H. Tataria, J. Musser, and P. Finamore, "Cycle-life model for graphite-$LiFePO_4$ cells," *J. Power Sources*, vol. 196, no. 8, pp. 3942–3948, Apr. 2011.

[27] H. Borhan, M. A. Rotea, and D. Viassolo, "Optimization-based power management of a wind farm with battery storage," *Wind Energy*, vol. 16, no. 8, pp. 1197–1211, 2013.

[28] P. Wolfs, "An economic assessment of 'second use' lithium-ion batteries for grid support," in *Proc. 20th Australas. Universities Power Eng. Conf.*, Dec. 2010, pp. 1–6.

[29] H. Bindner *et al.*, "Lifetime modelling of lead acid batteries," Risø Nat. Lab., Roskilde, Denmark, Tech. Rep. Risø-R-1515, Apr. 2005.

[30] C. Abbey and G. Joos, "A stochastic optimization approach to rating of energy storage systems in wind-diesel isolated grids," *IEEE Trans. Power Syst.*, vol. 24, no. 1, pp. 418–426, Feb. 2009.

[31] M. Saffari, M. S. Misaghian, D. Flynn, M. Kia, V. Vahidinasab, M. Lotfi, J. P. S. Catalao, and M. Shafie-Khah, "Multi-objective optimisation of an active distribution system using normalised normal constraint method," in *Proc. IEEE Milan PowerTech*, Jun. 2019, pp. 1–6.

[32] V. Vahidinasab and S. Jadid, "Stochastic multiobjective self-scheduling of a power producer in joint energy and reserves markets," *Electr. Power Syst. Res.*, vol. 80, no. 7, pp. 760–769, Jul. 2010.

[33] S. A. Bozorgavari, J. Aghaei, S. Pirouzi, V. Vahidinasab, H. Farahmand, and M. Korpås, "Two-stage hybrid stochastic/robust optimal coordination of distributed battery storage planning and flexible energy management in smart distribution network," *J. Energy Storage*, vol. 26, Dec. 2019, Art. no. 100970.

[34] M. Nick, R. Cherkaoui, and M. Paolone, "Optimal allocation of dispersed energy storage systems in active distribution networks for energy balance and grid support," *IEEE Trans. Power Syst.*, vol. 29, no. 5, pp. 2300–2310, Sep. 2014.

[35] H. Liang, G. Liu, H. Zhang, and T. Huang, "Neural-network-based event-triggered adaptive control of nonaffine nonlinear multiagent systems with dynamic uncertainties," *IEEE Trans. Neural Netw. Learn. Syst.*, vol. 32, no. 5, pp. 2239–2250, May 2020.

[36] H. Liang, X. Guo, Y. Pan, and T. Huang, "Event-triggered fuzzy bipartite tracking control for network systems based on distributed reduced-order observers," *IEEE Trans. Fuzzy Syst.*, vol. 29, no. 6, pp. 1601–1614, Jun. 2021.

[37] J.-H. Teng, "A direct approach for distribution system load flow solutions," *IEEE Trans. Power Del.*, vol. 18, no. 3, pp. 882–887, Jul. 2003.

[38] M. Abdel-Akher, K. M. Nor, and A. H. A. Rashid, "Improved three-phase power-flow methods using sequence components," *IEEE Trans. Power Syst.*, vol. 20, no. 3, pp. 1389–1397, Aug. 2005.

[39] Z. Yang, H. Zhong, A. Bose, T. Zheng, Q. Xia, and C. Kang, "A linearized OPF model with reactive power and voltage magnitude: A pathway to improve the MW-only DC OPF," *IEEE Trans. Power Syst.*, vol. 33, no. 2, pp. 1734–1745, Mar. 2018.

[40] H. Yuan, F. Li, Y. Wei, and J. Zhu, "Novel linearized power flow and linearized OPF models for active distribution networks with application in distribution LMP," *IEEE Trans. Smart Grid*, vol. 9, no. 1, pp. 438–448, Jan. 2018.

[41] T. Akbari and M. T. Bina, "Linear approximated formulation of AC optimal power flow using binary discretisation," *IET Gener., Transmiss. Distrib.*, vol. 10, no. 5, pp. 1117–1123, Apr. 2016.

[42] A. Ben-Tal and A. Nemirovski, "On polyhedral approximations of the second-order cone," *Math. Oper. Res.*, vol. 26, no. 2, pp. 193–205, May 2001.

[43] Trojan Battery Inc. (2021). *'TR 12.8-110-Li-Ion Battery*. [Online]. Available: https://trojanbattery.com

[44] S. Downing and D. Socie, "Simple rainflow counting algorithms," *Int. J. Fatigue*, vol. 4, no. 1, pp. 31–40, Jan. 1982.

[45] E. I. Vrettos and S. A. Papathanassiou, "Operating policy and optimal sizing of a high penetration RES-BESS system for small isolated grids," *IEEE Trans. Energy Convers.*, vol. 26, no. 3, pp. 744–756, Sep. 2011.

[46] (2021). *'Daily Radiation, Photovoltaic Geographical Information System*. [Online]. Available: http://re.jrc.ec.europa.eu

[47] (2021). *'Weather Underground: Local Weather Forecast*. [Online]. Available: https://www.wunderground.com

[48] Z. M. Salameh, B. S. Borowy, and A. R. A. Amin, "Photovoltaic module-site matching based on the capacity factors," *IEEE Trans. Energy Convers.*, vol. 10, no. 2, pp. 326–332, Jun. 1995.

[49] H. Kumar, S. Balasubramaniyan, S. Padmanaban, and J. Holm-Nielsen, "Wind energy potential assessment by Weibull parameter estimation using multiverse optimization method: A case study of Tirumala region in India," *Energies*, vol. 12, no. 11, p. 2158, 2019.

[50] S. Ali, S.-M. Lee, and C.-M. Jang, "Statistical analysis of wind characteristics using Weibull and Rayleigh distributions in Deokjeok-do Island–Incheon, South Korea," *Renew. Energy*, vol. 123, pp. 652–663, Aug. 2018.

[51] A. K. Jain, "Data clustering: 50 years beyond K-means," *Pattern Recognit. Lett.*, vol. 31, no. 8, pp. 651–666, 2008.
[52] T. Kanungo, D. M. Mount, N. S. Netanyahu, C. D. Piatko, R. Silverman, and A. Y. Wu, "An efficient *k*-means clustering algorithm: Analysis and implementation," *IEEE Trans. Pattern Anal. Mach. Intell.*, vol. 24, no. 7, pp. 881–892, Jul. 2002.
[53] B. Venkatesh, R. Ranjan, and H. B. Gooi, "Optimal reconfiguration of radial distribution systems to maximize loadability," *IEEE Trans. Power Syst.*, vol. 19, no. 1, pp. 260–266, Feb. 2004.
[54] PJM Learning Center. (2021). *'How Energy Use Varies With the Seasons*. [Online]. Available: https://learn.pjm.com
[55] 'PJM Interconnection LLC. (2021). *Day-Ahead Hourly LMPs*. [Online]. Available: https://dataminer2.pjm.com
[56] (2021). *'A Behind the Scenes Take on Lithium-Ion Battery Prices*. [Online]. Available: https://about.bnef.com
[57] A. Soroudi, *Power System Optimization Modeling in GAMS*, vol. 78. Cham, Switzerland: Springer, 2017.

ALI SOLEIMANI received the B.Sc. degree in electrical engineering from the Shahid Chamran University of Ahvaz, Iran, in 2016, and the M.Sc. degree in electrical engineering from Shahid Beheshti University (SBU), Tehran, Iran, in 2020.

His research interests include distribution system operation, renewable energy sources, electric vehicle integration, energy storage systems, and machine learning applications in power networks.

VAHID VAHIDINASAB (Senior Member, IEEE) received the Ph.D. degree in electrical engineering from the Iran University of Science and Technology, Tehran, Iran, in 2010.

He is currently an Assistant Professor (U.K. Senior Lecturer) of electrical power engineering and the Director of GRIDLAB at Nottingham Trent University, Nottingham, U.K., where he leads teaching and research in the area of sustainable power and energy systems. Before that, he was an Assistant Professor at Shahid Beheshti University, Tehran, and a Senior Research Associate at the EPSRC National Centre for Energy Systems Integration, Newcastle University, Newcastle upon Tyne, U.K., where he worked on the EU Horizon 2020 inteGRIDy Project and Active Building Centre (ABC) Research Programme. From 2011 to 2018, he held a number of leadership roles at SBU and the Niroo Research Institute. He has demonstrated a consistent track record of attracting external funds and managed industrial projects and closely worked with 12 large and complex national/international projects. His research works have been funded by the U.K. EPSRC, EU-H2020, and industry partners and local utilities of U.K. and Iran. His research interests include power and energy systems modeling, analysis and control, smart grids, energy systems integration, and energy markets.

Dr. Vahidinasab is a member of the IEEE Power and Energy Society (PES) and the IEEE Smart Grid Society. He is currently an Associate Editor of the IEEE Transactions on Industry Applications. He is also a member of the Editorial Board and a Subject Editor of the *IET Generation, Transmission and Distribution*, and an Associate Editor of the *IET Smart Grid*, *Nature Scientific Reports*, and IEEE Access. He was considered as one of the Outstanding Reviewers of the IEEE Transactions on Sustainable Energy in 2018 and IEEE Transactions on Power Systems in two consecutive years of 2020 and 2021.

JAMSHID AGHAEI (Senior Member, IEEE) received the B.Sc. degree in electrical engineering from the Power and Water Institute of Technology, Tehran, Iran, in 2003, and the M.Sc. and Ph.D. degrees from the Iran University of Science and Technology, Tehran, in 2005 and 2009, respectively. He is currently a Full Professor with the Lappeenranta–Lahti University of Technology (LUT), Lappeenranta, Finland. His research interests include smart grids, renewable energy systems, electricity markets, and power system operation, optimization, and planning. He was considered one of the Outstanding Reviewer of the IEEE Transactions on Sustainable Energy, in 2017. He was a Guest Editor of the Special Section on "Industrial and Commercial Demand Response" of the IEEE Transactions on Industrial Informatics, in 2018, and the Special Issue on "Demand Side Management and Market Design for Renewable Energy Support and Integration" of the *IET Renewable Power Generation*, in 2019. He is an Associate Editor of the IEEE Transactions on Smart Grid, the IEEE Systems Journal, the IEEE Transactions on Cloud Computing, the IEEE Open Access Journal of Power and Energy, and *IET Renewable Power Generation*, and a Subject Editor of the *IET Generation Transmission and Distribution*.